Accepted manuscript. Layout mimicks the paper to be published. N.S. 2003 04 07

Macromol. Chem. Phys. **2003** , *204(7)*, 1000-1013

Full Paper: The present paper discloses the changes in the nanostructure as revealed by small–angle X–ray scattering (SAXS) of synchrotron radiation of anisotropic semicrystalline samples of polyester and poly(ether ester) type differing in their chemical composition, while subjected to controlled progressive elongation. From the group of polyesters poly(ethylene terephthalate) (PET), and poly(butylene terephthalate) (PBT) were selected. Two PBT–based commercial poly(ether ester)s were also studied differing in the molecular weight of their soft segments (poly(tetramethylene glycol, PTMG) being 1000 (Arnitel® EM550) and 2000 (Arnitel® EM400), respectively. A blend of PBT and EM550 (40/60 by wt.) was also characterized. All materials underwent the same sample preparation process resulting in highly oriented "bristles" of 1 mm diameter. It was found that ε_b, the elongation at break, strongly depends on the flexibility of the glycol residues of the materials studied – ranging from ε_b = 8% for PET that contains ethylene glycol residues, through ε_b = 18% for PBT including the more flexible tetramethylene glycol (TMG) up to ε_b = 510% for the PEE containing the longest PTMG moieties. During straining the relationship between the external elongation ε and the changes in the long spacing L was determined. After relaxation from each deformation step the relationship between the tensile set ε_r and the long period L was also followed and discussed. Such analysis led to a model describing the nanostructure evolution during the deformation–relaxation cycle that finally was verified and refined utilizing the multidimensional chord distribution function (CDF) computed from the anisotropic SAXS patterns.

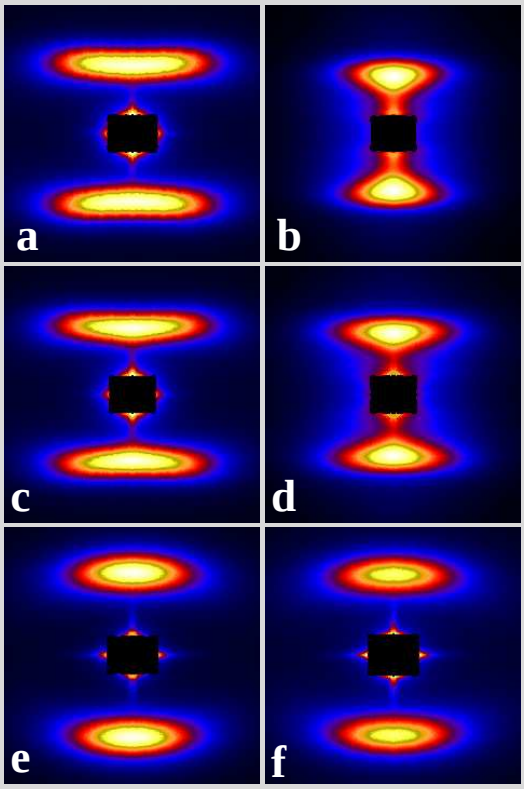

2D SAXS patterns (pseudo color) of bristles of PET (PBT), respectively, cold drawn, $\lambda = 3.5$ ($\lambda = 2.3$) and annealed with fixed ends for 6 h at 240 °C (180 °C), recorded at room temperature at a forced tensile deformation ε or tensile set (residual elongation) ε_r.

Deformation Behavior of PET, PBT and PBT-Based Thermoplastic Elastomers as Revealed by SAXS from Synchrotron

Norbert Stribeck[*1], *Stoyko Fakirov*[2], *Anton A. Apostolov*[2], *Zlatan Denchev*[3], *Rainer Gehrke*[4]

[1]Institute of Technical and Macromolecular Chemistry, University of Hamburg, Bundesstr. 45, 20146 Hamburg, Germany, Fax: +49 40-4123-6008, eMail: Norbert.Stribeck@desy.de
[2]Laboratory on Structure and Properties of Polymers, University of Sofia, 1126 Sofia, Bulgaria
[3]Department of Polymer Engineering, University of Minho, Campus Azurem, 4800–058 Guimarães, Portugal
[4]HASYLAB at DESY, Notkestr. 85, 22603 Hamburg, Germany

Keywords: elastomers; SAXS; strain; synchrotron radiation; thermoplastics

Introduction

Poly(ether ester) block copolymers exhibit an extraordinary combination of elasticity, toughness, low temperature flexibility, and strength at 150°C. They are now of great commercial importance as engineering type thermoplastic elastomers. This set of properties is related mainly to the existence of cross-links tying the array of macromolecules into an infinite network. In

natural rubber and synthetic elastomers these crosslinks represent chemical bonds. In thermoplastic elastomers, thermally labile tie points held together by physical forces replace them. These junctions may be glassy, crystalline or even hydrogen bonded molecules or ionic associates.[1]

In order to behave as a thermoplastic elastomer, the molecules must contain two types of units, blocks or chains segments forming a soft and a hard phase. The soft chain segments form an amorphous phase (above the glass transition temperature T_g). They impart elastomeric character to the copolymer whereas the hard blocks are capable of intermolecular association with other hard blocks; they should form a solid phase in the service temperature range in order to impart dimension stability to the array of molecules. At high temperature, dissociation of the physical bonds occurs. The soft and hard blocks may be arranged in various ways, randomized or ordered. Their way of ordering affects the physical and mechanical properties of the material.[1,2]

Thermoplastic elastomers are an attractive object for structural investigations not only because of their peculiar mechanical properties, but also because they offer many modeling opportunities due to their crystallizability, multiblock character and possibility of varying both the block flexibility and length. There are also a lot of unanswered questions concerning the deformation mechanism of this class of polymers as compared to classical rubbers. For this reason the relationship between macro- and microdeformation was systematically studied during the last decade[3–9] by means of small-angle X-ray scattering (SAXS). All studies were carried out on polyblock poly(ether esters) (PEE) consisting of poly(butylene terephthalate) (PBT) as hard segments and poly(ethylene glycol) (PEG) as soft segments in different ratios. Mostly PBT/PEG(1000) 49:51 by wt. was the starting material. In the sample designation the number in parentheses indicates the average molecular weight of the PEG segments of the copolymer. The composition is indicated in the postfix. So-called "bristles" were prepared by first drawing ($\lambda = 5$) and then annealing the material with fixed ends at 170 °C in a vacuum for 6 h. Measurements were performed with or without application of stress on high power X-ray sources,[3–9] resulting in high-resolution two-dimensional (2D) SAXS patterns. Development of methods for the evaluation of such patterns has been regarded as well.[10–14]

In our early SAXS studies[3] on such samples a directly proportional increase of the long spacing L with the applied strain was found for a relative elongation $\varepsilon < 100\%$. At higher elongation pulling out of tight tie molecules from adjacent microfibrils occurs and some of the tie microfibrils relax, leading to appearance of two coexisting long periods. A model was suggested that described the behavior of the polymer system under and after application of stress.[3]

In subsequent investigations[4,5] the model was successfully applied to characterize the changes in the SAXS patterns of a set of 6 different PBT/PEG poly(ether esters) varying in their hard-to-soft segment ratio. By means of results from a two-dimensional (2D) detector it was possible to advance the model, revealing finer details in the copolymer nanostructure.[5] So at low macrodeformations two-point SAXS pattern of the oriented PBT/PEG segmented block copolymer were obtained. It was accepted that the morphology of the neat bristle represents assemblies of parallel crystalline lamellae oriented perpendicularly to the draw direction. The four-point patterns observed in the relaxed, unloaded state were explained by a zigzag arrangement of lamellae, the crystalline layers being tilted with respect to the straining direction. The observed morphological transition was found to be reversible and emerged more and more as the reversing deformation was increased in the series of straining cycles.[5]

A recent SAXS study[6] with data from a rotating anode indicated the occurrence of a complex "six-point" SAXS pattern in both stressed and relaxed bristles. Applying computerized graphical analysis of the patterns, we obtained indirect evidence of a six-point diagram.

Utilizing synchrotron radiation[9] two-, four- and unique six-point small-angle patterns as well as the corresponding transitions were clearly recorded. Five deformation intervals, dependent on the elongation level, were identified for the thermoplastic elastomer in question. The variation of the 2D scattering pattern in the straining cycles resulted in clear evidence concerning the six-point pattern by demonstrating that it is arising from two basic morphological ensembles related to the two- and the four-point fraction of the pattern, respectively. The former are related to relaxed stacks of domains detached from the elastic network, and the latter to domains integrated into it by tie-molecules still operating. This appears to be the only plausible explanation, because the peak position of the two-point feature of the SAXS pattern did not respond to the cycling strain, whereas the four-point feature did so and, moreover, the four-point feature vanished more and more as the reversing deformation was increased in the series of straining cycles.[12]

It was concluded that the preoriented polymer bristle can be considered a bunch of microfibrils that scatter independently for low deformations. For higher deformations, these microfibrils correlate in the transverse direction, too, and the interfibrillar distance was calculated in this case.

There are two goals of this study. Applying the same approach – namely following the relationship between macro- and microdeformation by means of SAXS recorded during the measurement under and without stress we intend (i) to investigate the behavior of commercial PEE comprising as soft segments poly(tetramethylene glycol) (PTMG), and (ii) to investigate the behavior of the neat PET and PBT as well as the blend PBT/PEE and to compare them with the results, obtained earlier.[3–9] Such a comparison will shed light on the validity of the models derived from PEE with PEG-based soft segments[3–9] and will help to better understand the contribution of PBT hard segment to the entire behavior of PEE.

Experimental Part

Materials

Commercial, engineering grade PET (Yambolen, Bulgaria) and PBT (Aldrich Chemical Company, melt index = 50) were used as homopolymers. Two PEEs (Arnitel®, DSM, The Netherlands), designated as EM400 and EM550, with molecular weight/weight content of the PTMG soft segments 2000/60 and 1000/35, respectively, were used independently and in the blend with PBT. Before preparing the blend the component materials were finely ground and dried at 100°C for 24 h. The blend itself was obtained by mixing of PBT and EM550 in a ratio of 40:60 by wt. The blend components are immiscible. Bristles having approximate diameters of 2 mm were obtained using a Melt Flow Index apparatus (MFI-6542, Donau Electronics, Switzerland) at appropriate temperature, depending on the polymer. The melt was kept in the barrel for approx. 10 min and subsequently extruded through the nozzle (2 mm diameter) into ice-cold water by applying a constant force of 220 N to the plunger.

The as extruded bristles were drawn in a tensile testing machine (Zwick 1464) at room temperature and a strain rate of 20 mm · min^{-1} to a draw ratio λ = 3.6–4.0, which resulted in a final diameter of about 1 mm, followed by annealing for 6 h with fixed ends in a vacuum oven at 210 °C for PET, 180 °C for PBT, 170 °C for PEE and the blend PBT/PEE.

Methods

Small-angle X-ray scattering measurements under stress were performed using a frame allowing controlled variation of the sample length. Each measurement under stress was followed by one in the absence of stress (in the "relaxed state") before a larger deformation was applied in the subsequent cycle. Thus, the samples were studied in various deformation ranges, depending on their extensibility which was as high as 500% for the PEE EM400. Here an in the following, the elongation ε in percent is defined as: $\varepsilon = 100 \times (\ell - \ell_0)/\ell_0$, where ℓ_0 and ℓ are the initial and the actual bristle length, respectively, as measured between two marks close to the irradiated part of the bristle. In the case of measurements in the relaxed state, the same equation was used to compute the residual elongation ε_r.

The patterns from the relaxed samples are denoted, for example, as ε_r = 4.7(8), where the first number represents the tensile set (i.e. the residual plastic deformation), ε_r, after straining to a tensile deformation, ε, given by the number in parentheses.

Synchrotron radiation (λ=0.15 nm) generated at the beamline A2 of HASYLAB, Hamburg, Germany was applied. The sample-to-detector distance was set to 180 cm. Diffraction patterns were registered by means of a 2D image plate detector. The exposure time was 2 min. An area of 900 × 900 pixels, each with a size of 176 × 176 μm was read out and used for evaluation. After each exposure under stress the sample was released while the detector plate was exchanged during the following minute. After that another exposure was carried out while the macroscopic shrinking process of the sample was still going on. Thereafter, again, the image plate was exchanged and the sample was drawn to the subsequent elongation step in the series. Immediately after that a new cycle started. Thus, patterns under stress and patterns after relaxation were recorded as a function of an increasing external deformation. Unfortunately each plate was aged differently, and a a new but slow image plate scanner had to be used. So there was no chance to perform a common background subtraction or to track the intensities of the patterns with respect to each other. For the determination of long periods from peak maxima this is no problem, but for a quantitative analysis of SAXS intensity it is. Nevertheless, by automatic iterative spatial frequency filtering it is still possible to extract the nanostructure information from the SAXS, after suitable transformation to display it as a multidimensional chord distribution function (CDF), and finally to discuss it.[11,13,15,16] The discussion is straightforward, since the CDF has been defined[11] by the Laplacian of Vonk's multidimensional correlation function.[17] As such it presents the autocorrelation of the surfaces from the (nanosize) domains in space in a similar manner as Ruland's interface distribution function does[18–20] for one-dimensional structures as a function of distance. For samples with fiber symmetry the CDF $z(r_{12}, r_3)$ is a function of two co-ordinates only (transverse direction r_{12} and the fiber direction r_3). Therefore it can be displayed by means of contours in a plane. Positive peaks found in the vicinity of the origin are size distributions of the primary domains. Thus their size, shape and orientation in space are depicted. Negative peaks following farther out exhibit "long periods", i.e. the distance of two adjacent domains from each other. Following positive peaks describe the size and orientation of superdomains (i.e. assemblies made from two primitive domains separated by a rather probable distance and measured from the beginning of the first to the end of the second domain), and correlations among domains more distant are manifested in consecutive peaks at longer distance. As has been expatiated in several papers,[11,15,16] the CDF is computed from the scattering intensity $I(\mathbf{s})$ by

$$z(r_1, r_3) = -\mathscr{F}^2\left(4\pi^2\left(s_1^2 + s_3^2\right)\{I(\mathbf{s})\}_2(s_1, s_3) - B(s_1, s_3)\right), \quad (1)$$

with the projection of the scattering intensity on the representative (s_1, s_3)-plane,

$$\{I(\mathbf{s})\}_2(s_1, s_3) = \int I(\mathbf{s})\, ds_2, \quad (2)$$

the factor $-4\pi^2\left(s_1^2 + s_3^2\right)$ being equivalent to the Laplacian in physical space, $B(s_1, s_3)$ describing a background determined by spatial frequency filtering of $4\pi^2\left(s_1^2 + s_3^2\right)\{I(\mathbf{s})\}_2(s_1, s_3)$, and $\mathscr{F}^2(\,)$ denoting a 2D Fourier transformation.

Results

Figures 1-7 display the results taken from the homopolymers PET and PBT, of the commercial thermoplastic elastomer of PEE type comprising PTMG as soft segments, of the blend PBT/PEE and two types of the same PEE differing in their hard-to-soft segment ratios. The results are represented as 2D scattering patterns and as graphs showing the long spacings L as a function of the elongation (ε or ε_r). The L values were calculated by means of the Bragg's law from the positions of the peak maxima of both two- and four-point scattering patterns. The results shown in Figures 1-7 represent the two basic states of the samples – both under stress as a function of the tensile deformation, ε, and after relaxation as a function of the residual deformation, ε_r.

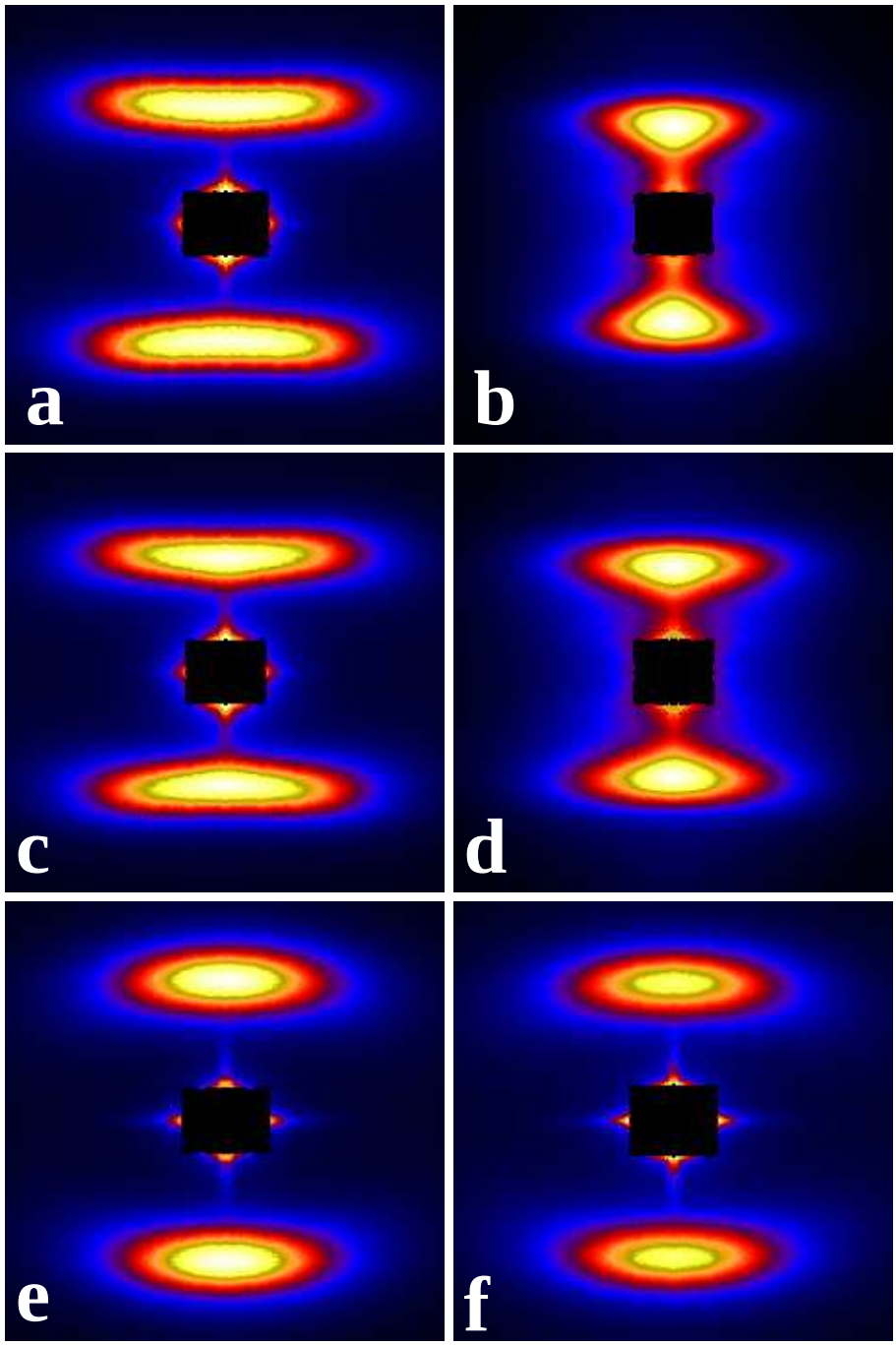

Figure 1: 2D SAXS patterns (pseudo color) of bristles of PET (PBT), respectively, cold drawn, $\lambda = 3.5$ ($\lambda = 2.3$) and annealed with fixed ends for 6 h at 240 (180°C), recorded at room temperature at a forced tensile deformation ε or tensile set (residual elongation) ε_r in percent as follows: (a) PET, $\varepsilon = 0$; (b) PET, $\varepsilon = 8$; (c) PET, $\varepsilon_r = 0(5.5)$; (d) PET, $\varepsilon_r = 4.7(8)$; (e) PBT, $\varepsilon = 0$; (f) PBT, $\varepsilon_r = 6.7(16.7)$. The value in parentheses is the forced elongation in percent during the previous measurement under stress. Each square covers the range $-0.15\,\mathrm{nm}^{-1} < s_{12}, s_3 < 0.15\,\mathrm{nm}^{-1}$ with the modulus of the scattering vector defined by $s = \left(s_{12}^2 + s_3^2\right)^{0.5} = (2/\lambda)\sin\theta$. Straining direction is vertical.

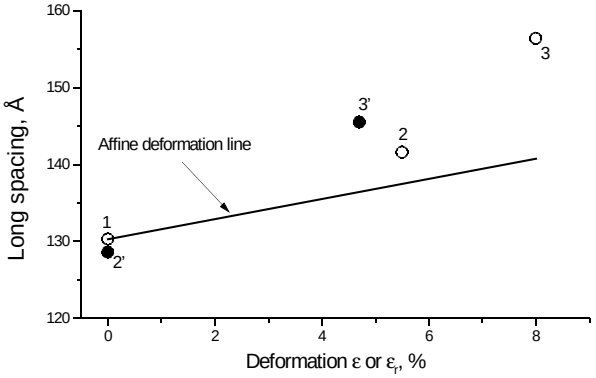

Figure 2: Long spacing L calculated from two–point patterns, *vs.* elongation ε or ε_r for the PET homopolymer: open circles – samples under stress ($L(\varepsilon)$) ; solid circles – sample in relaxed state ($L(\varepsilon_r)$). The digits show the sequence of the measurements with the progress of the external elongation ε. The "primed" digits depict measurements without stress at $\sigma = 0$ at the respective residual elongation ε_r.

Unfortunately, due to the shortcomings of the available image plate detector system, it was impossible to obtain reliable information on the effect of deformation on the variation of the total scattering intensity. For this reason corresponding statements are missing in the present study in contrast to previous ones[3–8] performed with conventional X-ray sources.

Let us look at the presented results in the sequence defined by the increasing flexibility of the "soft" chain constituents of the materials studied, i.e., PET, PBT, PBT/PEE, PEE EM550, and PEE EM400. Such a presentation allows one to follow the effect of the chain flexibility on the relationship between macro- and microdeformation, the latter being expressed by the variations of L in the stressed ($\sigma \neq 0$) and relaxed ($\sigma = 0$) states.

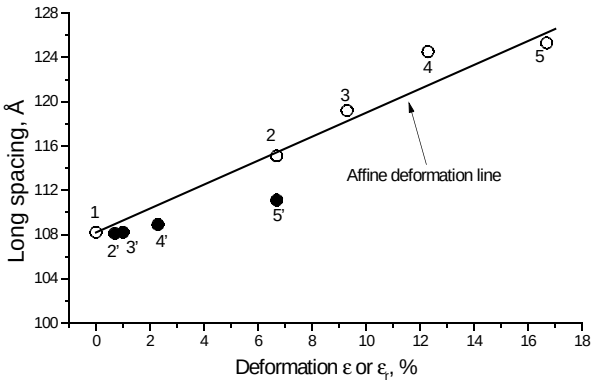

Figure 3: Long spacing L calculated from two–point patterns, *vs* elongation ε or ε_r for the PBT homopolymer: open circles – samples under stress; solid circles – sample in relaxed state. The meaning of the digits is the same as in Figure 2.

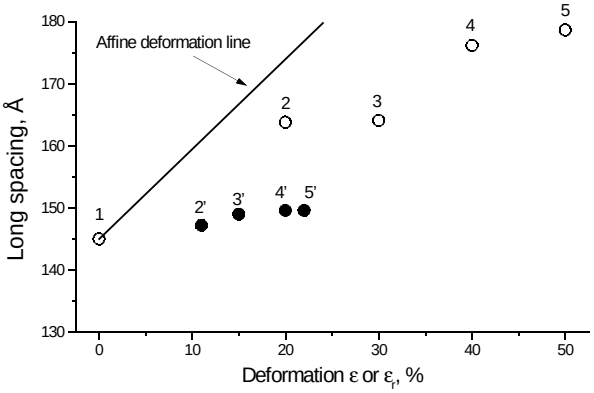

Figure 4: Long spacing L calculated from two–point patterns *vs* elongation ε or ε_r for the blend of PBT/PEE 40:60 wt.-% (PEE is Arnitel® EM550): open circles – sample under stress; solid circles – sample in relaxed state. The meaning of the digits is the same as in Figure 2.

Figure 1 shows selected SAXS patterns from the deformation-relaxation cycles at different forced (ε) or residual (ε_r) deformations for bristles of PET and PBT homopolymers cold drawn and annealed with fixed ends. It is important to note that the type of the scattering patterns is the same for the two homopolymers, regardless of the extent and character of deformation (ε or ε_r), namely all the patterns are of the two-point type. What is changed during these measurements is the shape of the peaks and the distance between the two reflections, which indicates variation of the long spacing with the progress of deformation. These changes are better expressed in the next two figures demonstrating the effect of the level and character of deformation on L. Before discussing these results, let us point out the important difference in the behavior of the two homopolymers. While PET breaks after the measurement at ε = 8% ($\varepsilon_b > 8\%$), PBT displays twice the elongation at break.

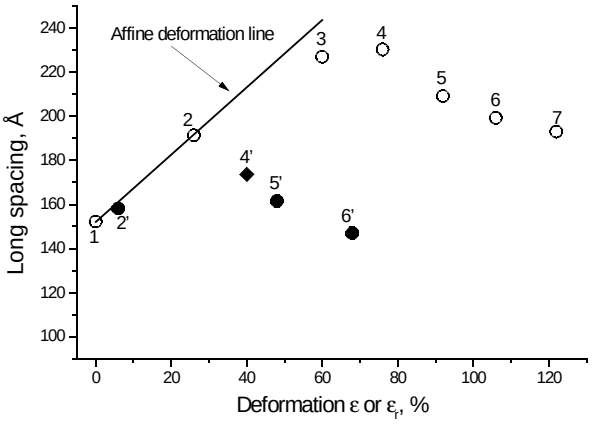

Figure 5: Long spacing L calculated from two- and four–point patterns *vs* elongation ε or ε_r for sample PEE (Arnitel® EM550): open circles – sample under stress; filled circles – sample in relaxed state; filled diamond – sample in relaxed state, (L calculated from four–point pattern). The meaning of the digits is the same as in Figure 2.

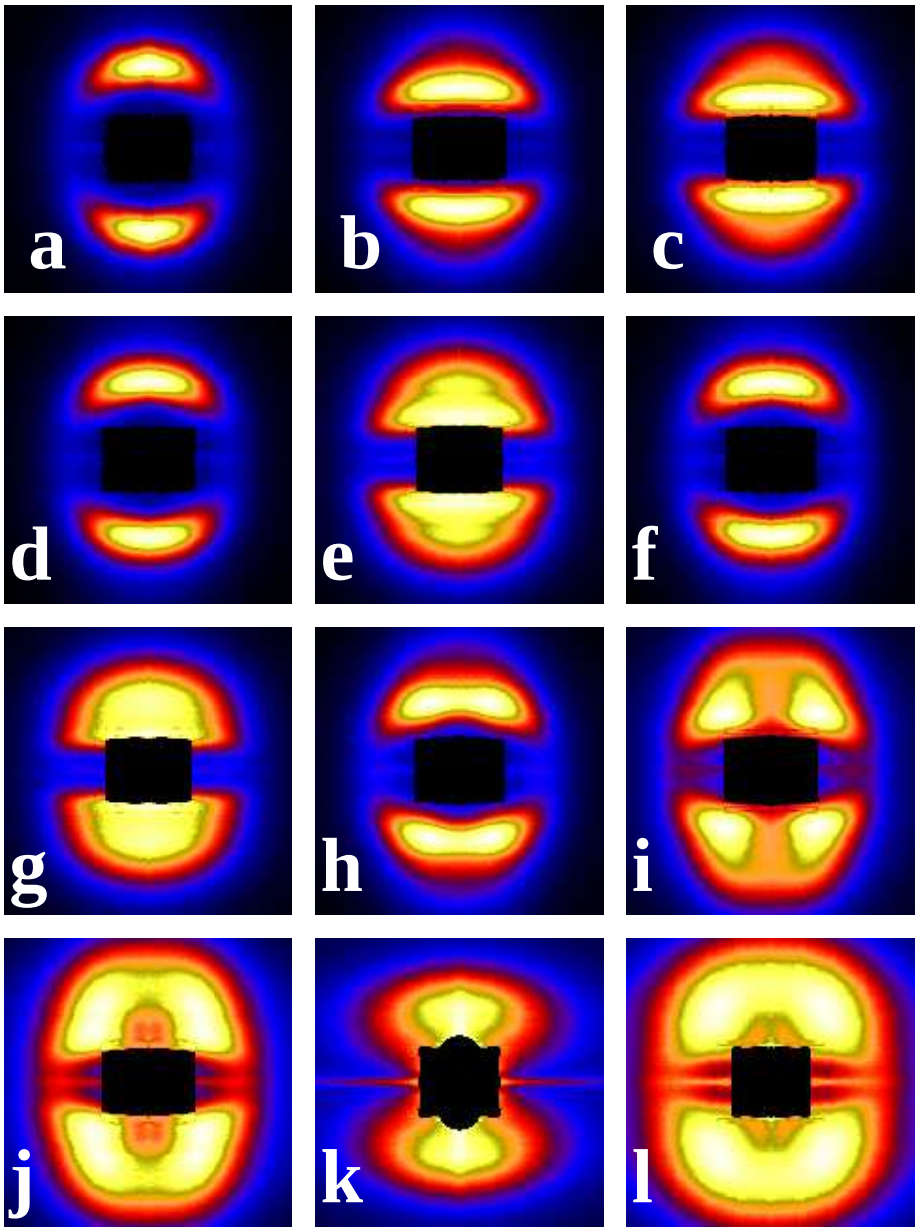

Figure 6: 2D SAXS patterns (pseudo color) of bristle of PEE (Arnitel® EM400) cold drawn (λ = 2.3) and annealed with fi xed ends for 6 h at 180°C , collected in the strained (elongation ε in percent) or the relaxed (tensile set ε_r in percent) state, respectively: (a) ε = 0; (b) ε = 0(50); (c) ε = 80; (d) ε_r = 25(80); (e) ε = 100; (f) ε_r = 25(100); (g) ε = 140; (h) ε_r = 25(140); (i) ε_r = 51(250); (j) ε_r = 106(360); (k) ε = 510; (l) ε_r = 205(510). The value in parentheses is the elongation in percent during the previous measurement under stress. Each square covers the range $-0.1\ \mathrm{nm}^{-1} < s_{12}, s_3 < 0.1\ \mathrm{nm}^{-1}$ with the modulus of the scattering vector defi ned by $s = \left(s_{12}^2 + s_3^2\right)^{0.5} = (2/\lambda)\sin\theta$. Straining direction is vertical.

Figure 2 shows the dependence of L as a function of the forced ($\sigma > 0$) elongation ε and residual ($\sigma = 0$) elongation ε_r for PET. Figure 3 represents the same dependence for PBT homopolymer. Obviously the experimental points for PET (Figure 2) are rather scattered for the two kinds of measurements ($\sigma > 0$ and σ = 0). For this reason it is impossible to derive any well-defined relationship between deformation and long spacing value. Nevertheless, there are two noteworthy results. First, a completely reversible response of $L(\varepsilon, \varepsilon_r)$ upon cycling the strain up to ε = 5.5% (Figure 2, points 2, 2') is observed, whereas there is only partial reversibility at higher deformations. Second, comparing the increase of the long spacing for PET and PBT (Figures 2 and 3), it is observed that for the same elongation interval ε the increase of L for PET is approximately twice that for PBT (Figures 2 and 3).

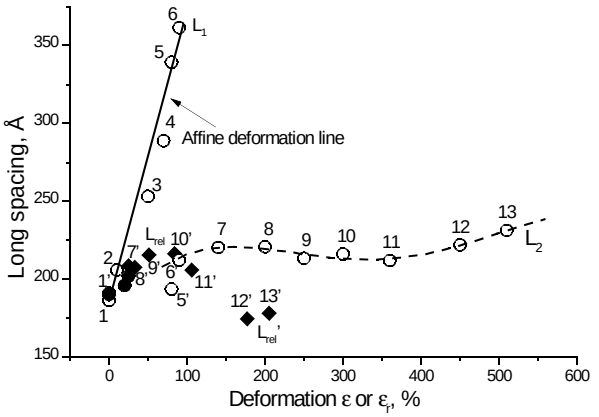

Figure 7: Long spacing L *vs* deformation ε or ε_r for a PEE sample (Arnitel® EM400): open circles – sample under stress; filled circles – sample in relaxed state; filled diamonds – sample in relaxed state, (L calculated from four-point pattern). The meaning of the digits is the same as in Figure 2.

Quite different is the behavior of PBT displayed in Figure 3. As compared to PET, the dependence of L on the external macrodeformation can be followed in a deformation interval twice longer – up to $\varepsilon_b > 18\%$. Moreover, in the entire interval of ε a very well expressed linear relationship is observed between the macro- (ε) and microdeformation (L). The respective line coincides with that of the affine deformation model, and the deformation is completely reversible up to $\varepsilon = 12\%$.

The similarity of the PET and PBT scattering patterns on the one hand, and the differences between their deformational behavior on the other hand (Figure 2 and 3, respectively), i.e., their macrodeformation limits, the reversibility of deformation and its character (affine or non-affine) lead to a preliminary conclusion regarding the reason for the differences observed. It can be attributed to the different chemical composition – replacement of the ethylene glycol (EG) moieties of PET by the longer and more flexible tetramethylene glycol (TMG) units of PBT.

Let us now examine the deformational behavior of samples containing more flexible segments, those of poly(tetramethylene glycol) (PTMG) found in the thermoplastic elastomer of the poly(ether ester) type. But before looking on the neat PEE, the behavior of a 40:60 by wt. PBT/PEE blend comprising TMG and PTMG, respectively, will be considered.

The 2D SAXS scattering patterns (not shown) are similar to those presented in Figure 1, i.e., all of them are of the two-point type, regardless of the extent and kind of deformation (ε or ε_r). The dependence of the long spacing L on the deformation for the same PBT/PEE blend is shown in Figure 4. Most remarkable is the fact that for the blend the elongation at break, $\varepsilon_b = 50\%$ is much higher than those of the neat PET and PBT samples (Figure 2 and 3). Another difference, especially as far as PBT is concerned, is the character of macrodeformation under stress. Although L increases with ε more of or less linearly, the increase is significantly lower than the prediction of an affine microdeformation.

A common feature of the PBT/PEE blend (Figure 4) and the neat PBT (Figure 3) is the reversibility of the L values measured under and without stress. The corresponding values for the measurements without stress are close to the initial one, although the tensile set ε_r increases with the progress of the forced elongation ε and becomes almost the half of the latter ($\varepsilon_r \approx \varepsilon/2$), similar to earlier studied PEE samples comprising PEG as soft segments.[3–6]

The next sample of the series is the commercial thermoplastic elastomer Arnitel® EM550 comprising as soft segments 35 wt.-% of PTMG. The dependence of L on ε and ε_r for this sample is plotted in Figure 5. The 2D SAXS patterns obtained from this sample are again of the two-point type, as those shown in Figure 1, with the exception of the pattern at ε_r = 40% where one observes a trend toward the formation of a four-point diagram, similarly to the next sample (Figure 6) and in accordance with the reports for PEE based on PBT and PEG.[3–9]

What is interesting with this neat PEE is its much higher extensibility. This material breaks at ε_b = 120%. Furthermore, $L\,(\varepsilon)$ shows an almost linear increase up to ε = 50% and obeys the affine model of deformation. At ε = 70% the L value starts to drop significantly, again following a nearly linear dependence. Concerning the L values measured without stress, they are close to the initial one at $\varepsilon = 0$ (Figure 5). Even more, the value obtained at ε_r = 70% is slightly below the initial one as found in earlier studies for PEE comprising PEG as soft segments.[3–5]

The last sample also represents a PEE (Arnitel® EM400) including PTMG as soft segments (PBT/PTMG 40:60 by wt.). It should be stressed immediately that its deformation behavior is completely different from that of all previous samples. First, its extensibility is extremely high as compared to the previous materials (Figure 2–5) reaching $\varepsilon_b = 510\%$. Second, the scattering patterns in this large deformational interval vary in type – there are both two-point and four-point diagrams. Selected 2D scattering patterns are displayed in Figure 6.

Analyzing all of these patterns taken in the interval of ε between 0 and 510% under stress (12 patterns), one can define three deformational ranges characterized by different types of scattering patterns. In the first interval of deformations (ε = 0 – 80%) the scattering patterns are of the two-point type no matter if they are taken under or in the absence of stress (Figure 6, ε = 0 up to 80%). In the second deformation interval (ε = 80 – 140%) the scattering patterns are again of the two-point type but a second long spacing is observed when the sample is under stress. (Figure 6, ε = 100 and 140%).

Such a coexistence of two long periods has been found earlier in similar investigations of PEE comprising PEG as soft segments.[3–9]

In the third deformational interval (ε = 140 - 510%) the two-point scattering patterns are present only in the measure-

ments carried out under stress. Those taken in the relaxed state are distinguished by perfect four-point shape (Figure 6, ε_r = 25(140) up to 205(510)).

The results of the quantitative determinations of the long spacings of all the patterns taken under stress ($\sigma \neq 0$) or in the absence of stress (σ = 0) are presented in Figure 7. The majority of L values are obtained from two-point patterns (Figure 7, ∘ •), and the rest from four-point patterns (Figure 7, diamonds◊ ⧫). The data in Figure 7 demonstrate also a rather different deformation behavior of this sample in comparison to that of the other ones (Figure 2–5). The very high elongation at break has already been discussed. Further, the L values measured as a function of the forced (ε) or residual deformation (ε_r) formulate at least three well-expressed tendencies. Up to ε = 80-100%, L increases linearly with ε, the straight line being quite close to that reflecting the affine deformational model. In this interval of ε, the long spacing measured under stress is almost doubling, whereas the corresponding values in the absence of stress (σ = 0) are very close to the initial one (Figure 7, points 2*I* – 5*I*). This means that the macrodeformational changes provoked by the external deformation ε are completely reversible. This conclusion is supported by the observation that up to a total deformation of ε = 50% ε_r is close to zero (Figure 7).

In the intermediate deformation interval (ε = 80 – 140%) a tendency towards simultaneous formation of two long spacings is observed. This was already demonstrated when discussing the 2D SAXS patterns (Figure 6). This result is not surprising. It has already been observed and interpreted for the case of PEE involving PEG as soft segments.[3–9]

With further progress of the external deformation (ε up to 510%), only one long spacing arising from the two-point patterns ($\sigma \neq 0$) or from four-point patterns (σ = 0) can be observed. Both of them are much smaller than that registered at lower deformation (L_1), being in the vicinity of the initial L value (L_0). Nevertheless, they differ in value while those measured under stress (L_2) remain constant with values slightly larger than L_0. For $\varepsilon_r \leq 100\%$ the measured relaxed long period L_{rel} shows values close to those of L_2. For the highest forced (ε = 450 and 510%) and residual (ε_r = 177 and 205%) deformations the values of L_{rel} are close to the initial value L_0 (Figure 7, diamonds).

Chord Distribution of the Neat EM400 Bristle

Finally, we present the multidimensional chord distribution functions (CDF) computed from the scattering patterns (Figure 6) as described in the Experimental Part. Figure 8 exhibits the nanostructure of the neat bristle from Arnitel® EM400 before straining. The fiber direction is vertical (r_3). r_{12} is the transversal direction in cylindrical co-ordinates. Figure 8a shows the elevated contours from the CDF that exhibit the domain nanostructure. The central pair of peaks (1) describes the basic domain structure. The elongated shape parallel to the equator indicates lamellae with an average diameter of 20 nm.

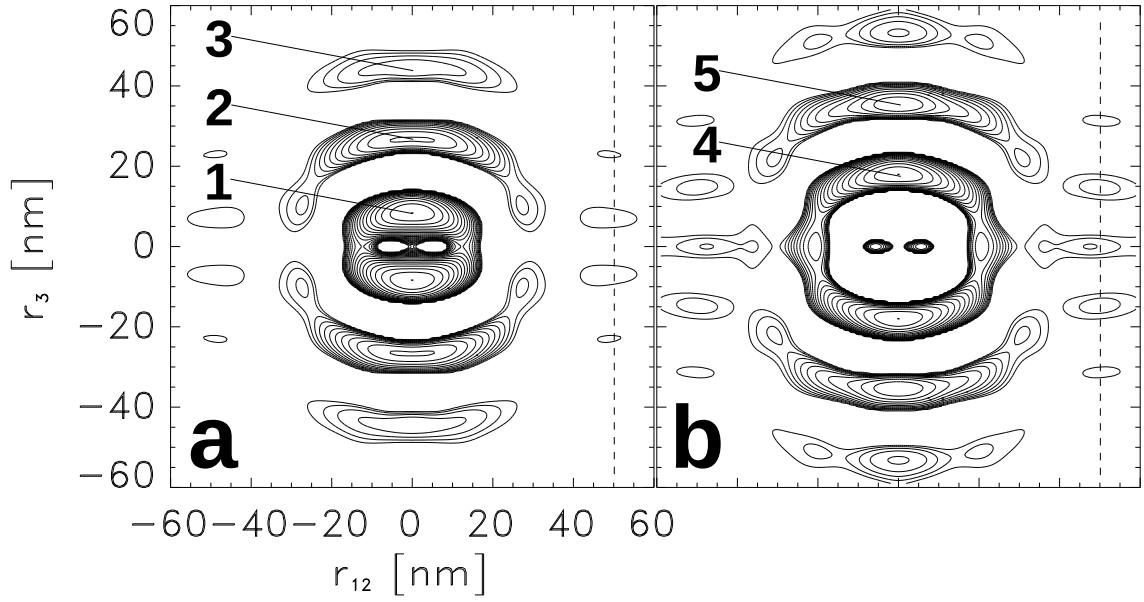

Figure 8: EM400 neat bristle. Chord distribution function (CDF, logarithmic scale) computed from 2D–SAXS pattern. Fiber direction is vertical. (a) Positive contours describing the domains from the nanostructure. (b) Negative contours describing the lattice properties.

The average layer thickness, as determined from the maximum on the meridian, is $d = 8.3\,\mathrm{nm}$. Both the soft- and the hard-domain layers contribute to this peak. The second peak (2) describes sandwiches made from two hard domains with a soft layer in between. We propose to address them by the term "bi-domains". The average bi-domain thickness is 26.6 nm, and tri-domains (3) with an average thickness of 44.3 nm are observed as well. There are fewer bi-domains than mono-domains, and even less tri-domains although in the contour plots they appear emphasized due to a logarithmic scaling of peak heights that was chosen for the reason of clarity. We observe that the diameter of those lamellae which are members of a stack and form bi- and tri-domains is higher (30 nm) than that of the average mono-layers. The number of stacks containing more than 3 lamellae is negligible. A dashed vertical line indicates a very weak lateral correlation among adjacent stacks that is as well present in the contours describing the lattice properties (Figure 8b). The most common lattice property is the long period peak (4). From the position of the maximum we determine $L = 18.0\,\mathrm{nm}$, which is in good agreement to the value directly extracted from the SAXS pattern (Figure 7). A second (5) and even a third long period peak are observed at 35.2 nm and 53.4 nm in fiber direction and describe correlations among phase boundaries that are placed at double and triple the "lattice constant", L. In general there is no long-ranging lattice in the studied material, and consequently the negative peaks in the CDF that are related to the lattice property are weaker by one order of magnitude than the positive peaks that describe the ensemble of nanosize domains.

In a résumé, the neat bristle comprises lamellae of hard- and soft domains that are oriented perpendicular to the fiber direction. The average layer thickness is 8 nm. The diameter of the lamellae is varying considerably. Extended layers with a diameter of 30 nm have formed stacks comprising not more than 3 members. Imperfect layers with diameters of less than 20 nm are more frequent than the extended ones. Their correlation with neighboring domains is low.

Nanostructure Evolution During Strain Cycling

Figure 9 presents the nanostructure evolution during the straining cycle as revealed in the CDF for low and medium elongation ($50\% \le \varepsilon \le 140\%$).

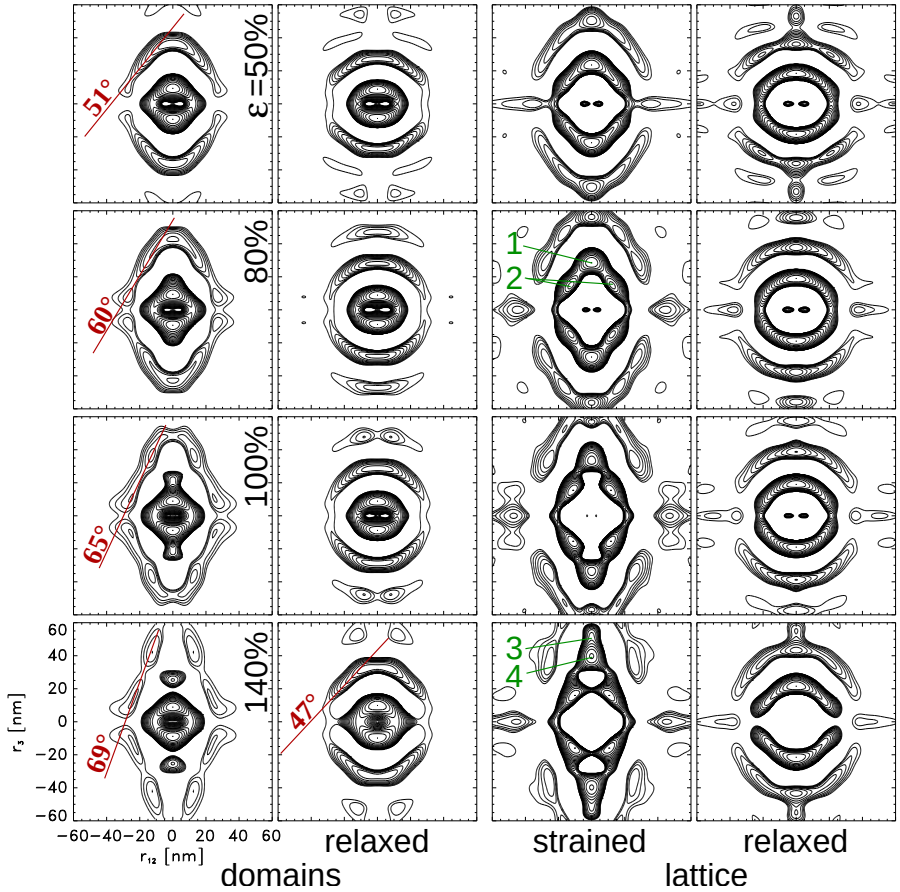

Figure 9: EM400 bristle in straining cycle. Lower elongations. Chord distribution function (CDF, logarithmic scale) computed from 2D–SAXS pattern. Fiber direction is vertical. Elongation $50\% \le \varepsilon \le 140\%$ as indicated in the left column. The contour plots of this column show the domain contours of the nanostructure in the strained states. The meaning of the other columns is given in the labels underneath.

The left column shows the chord distributions of the domains in the strained state. For all elongations the strong central domain peak exhibits a diamond shape that can be explained by the superposition of lamellae and other, rather compact mono-domains with a low aspect ratio. A separation by hand is impossible. Nevertheless, the bi-domain peak outside the central diamond is a set of four straight and elongated lines. To a first approximation it can be described by a (sub-)stack of two inclined lamellae. The increase of the tilt angle with increasing elongation from 51^{o} to 69^{o} is indicated in the plots. At 140% strain the linear peak begins to disintegrate into two parts indicating the formation of small domains by disruption of the lamellae. Beginning with an elongation of 100% two well-separated peaks of cylindrical soft- and hard-domains that are located in microfibrils are observed. The peak closer to the center is still constant and thus assigned to the hard domain cylinders with a height of 8.9 nm. The average height of the soft domains from the microfibrils is 21.3 nm at 100% and 25.1 nm at 140%. In the further course of the straining this soft domain height will not increase beyond 28 nm. Instead, the corresponding component will decrease and vanish indicating the maximum extensibility of the soft phase between two hard domains.

The second column shows the bristle in the relaxed state after the previous elongation. We observe a system of lamellar stacks with some orientation distribution about the meridian. Released from 140%, for the first time this orientation distribution of the bi-domains appears to be bimodal, with maxima of the preferential layer orientation at the meridian (0^{o}) and at $\approx 47^{o}$. There are no tri-domains with layer shape any more.

The third column shows the lattice peaks in the strained state. The long periods of the microfibrillar component (1) and of the tilted layers (2) are the most prominent features. Several higher orders are present. At $\varepsilon = 140\%$ we observe both a long period of microfibrils under tension (3) and a long period of relaxed microfibrils (4).

The fourth column shows the arrangement of long periods in the relaxed state. Up to the second order the long periods are clear and continuous, indicating an orientation distribution of lamellar stacks that contain not more than three layers.

Figure 10 presents nanostructure evolution during the straining cycle as revealed in the CDF for high elongation ($250\% \leq \varepsilon \leq 510\%$). For the strained state the first column reveals the transition from a macrolattice with hexagonal arrangement of small and compact domains into a pure microfibrillar system with perfect orientation.

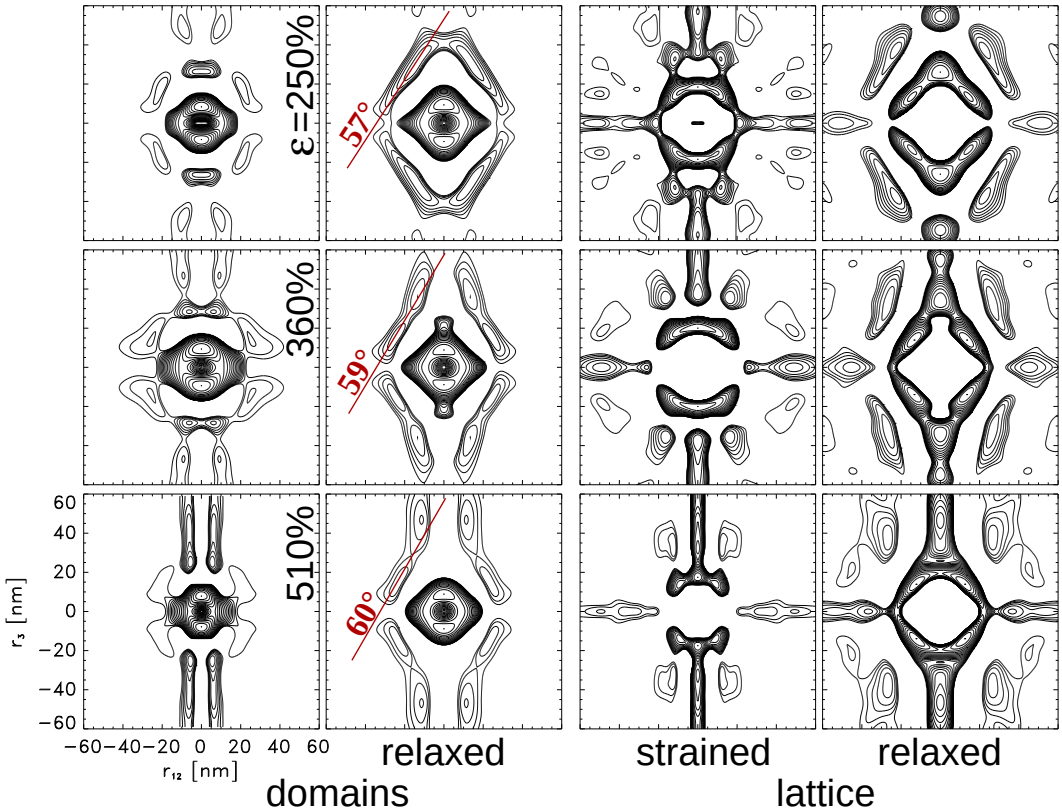

Figure 10: EM400 bristle in straining cycle. High elongations. Chord distribution function (CDF, logarithmic scale) computed from 2D–SAXS pattern. Fiber direction is vertical. Elongation $250\% \leq \varepsilon \leq 510\%$ as indicated in the left column. The contour plots of this column show the domain contours of the nanostructure in the strained states. The meaning of the other columns is given in the labels underneath.

The second column, again, shows the relaxed state. It is interesting to notice that, when releasing the stress, the disrupted domains again merge to form stacks of tilted lamellae. The inclination angle now is rather high and almost constant at 60^{o}. The diameter of these lamellae, again, is 30 nm. None of these stacks comprises more than 3 domains. The last two columns show the peaks related to the long periods in the strained and in the relaxed state. In the strained state (3rd column) the emerging microfibrillar component is clearly detected by the row of peaks on the meridian. Their strength is growing as the elongation increasing whereas a long period from some remnant lamellae oriented perpendicular to the fiber axis is vanishing.

Discussion

Effect of Chain Flexibility on the Deformational Behavior of PET, PBT, PEE and PBT/PEE Blend

The materials subjected to this investigation have a common characteristic feature with respect to their chemical composition. All of them can be viewed as being built from a rigid and a flexible part. For the two homopolymers PET and PBT the rigid part is the terephthalic acid residue, and for PEE it comprises the PBT hard segments. As to the flexible parts, these are ethylene glycol EG (for PET), tetramethylene glycol TMG (for PBT) and poly(tetramethylene glycol) PTMG (for the PEE). Obviously, the chain flexibility increases from EG to PTMG. This fact is reflected by the values of their glass transition temperatures, T_g, which are 70, 40 and $-50\,^{o}$C[21] (the last value is for a PEE comprising PEG as soft segments). Thus it is not surprising that the three polymers exhibit different limits of external deformations, including the blend PBT/PEE (Figure 2–6).

The different chain flexibility, or more precisely the flexibility of the "soft" part of the molecules, is responsible for the quite different fractions of the residual deformation, ε_r, from the total one, as well as the limit of ε below which the change of L is more or less completely reversible (Figure 2–5, 7). The flexibility of the "soft" parts strongly affects the character of microdeformation, making it to obey or disobey the affine model of deformation. The affine model of deformation can only be applied for the homo PBT and PEE Arnitel® EM400 (Figure 7).

Relationship Between Macro- and Microdeformation

The relationship between macro- and microdeformation is reflected in the relationship $L\,(\varepsilon)$. For PET (Figure 2) there is no well-defined relationship. For the other materials one observes a linear relation (Figure 3-5 and 7) that obeys the affine deformation model with the exception of the blend (Figure 4). At low elongations this increase is completely reversible, i.e. the L values measured in the corresponding deformational interval after removing the stress, are very close to the initial value L_0 (to be seen best in Figure 7).

In this context it is noteworthy to mention an early observation of Zhurkov *et al.*[22] on PA6 films. It has been demonstrated that the SAXS intensity increases continuously with drawing (ε = 12, 14 and 31%) during the measurement. Performing similar experiments, Fischer and Fakirov[23] showed that the scattering intensity is very sensitive to strain or stress for PET, too. For instance, measurements carried out on PET sheets of 1 mm thickness drawn five times and annealed at $260\,^{o}$C for 6 h have shown that the SAXS intensity increases sharply and reversibly when the sample is under strain (5–7%) at the time of measurement. If the strain is larger, the scattering intensity increases further but is no longer fully reversible.[23] Such reversibility (up to ε = 13%) was recently observed for PET in a PET/PE blend (50:50 by wt.)[24] by both the changes in L^{PET} and by the variation of the scattering intensity.[24]

The observed SAXS behavior of PET, either in the blend with PE[24] or as homopolymer,[23] as well as the changes of L for PET and particularly for PBT in the present case, i.e., the increase of the scattering intensity and/or the long spacing with extensional deformation, can be properly explained by the model proposed by Zhurkov *et al.*[22] assuming a density decrease of the soft (non-crystalline) phase due to its elongation. Such an explanation is supported by the fact of reversible change of both the intensity and L values for the respective deformational range. Their behavior suggests that the observed external elongation is related to conformational changes only in the amorphous domains, the crystallites remaining unaffected for these levels of deformation. This mechanism is proven in the case of PEE.[3–6, 14]

It should be stressed here that such an interpretation of the SAXS behavior (for both intensity and L) cannot be applied for example to PE in the above-mentioned PET/PE 50:50 by wt. blend. The possible reason for this is that the PE crystallites melt at much lower temperatures (around 120 compared to 255^{o}C for PET). In other words, their mechanical resistance during deformation is lower and during straining defects are introduced in crystallites leading to a decrease of the density difference between the hard and the soft phase that explains the observed continuous decrease of SAXS intensity of PE.[24]

Reversibility of the long spacing L in a certain range of lower macrodeformation is expressed in the best way by PBT (Figure 3) and by PEE Arnitel® EM550 (Figure 7) in this study. As discussed above it is related to conformational changes of the chains in the amorphous intercrystalline regions as repeatedly reported for similar[25] and other polymer systems.[26] This conclusion is supported by the observed changes of the shape of the 2D SAXS patterns themselves as shown in Figure 1 and 6 (up to ε = 80%). Application of stress in limited deformational ranges (ε up to 18% for homopolymers and up to 80% for PEE) causes the two-point reflections to get closer to one another and to move apart when stress is removed (Figure 1 and 6). These results suggest that at low deformation

levels no substantial persistent morphological changes occur – some of the morphological elements (ensembles of crystalline domains) remain the same as entire entities and keep their internal structure.

Let us now focus on the deformation behavior of the last sample, the PEE Arnitel® EM400, distinguished by the most typical properties for poly(ether ester)s (Figure 6 and 7). In addition to the behavior up to ε = 80% already discussed above, in the next range (ε = 80–140%), in contrast to the rest of the samples, a second periodicity (L_2) appears that coexists with the primary long spacing L_1 (Figure 6, ε = 100 and 140%, Figure 7). Such a second long spacing L_2 is reported for PEE comprising PEG as soft segments,[3,4] the effect having been explained by loosing of interfibrillar contacts in this interval of deformation. The result is relaxation of some microfibrils and the observation of a corresponding shorter long period L_2. With the further increase of the external deformation ε from 140 to 500%, the first periodicity L_1 disappears while L_2 remains constant. A more detailed description of the nanostructure evolution as a function of elongation is given in the description of the corresponding CDF features that reflects all the basic features given here, but adds quantitative data concerning the domain shapes and orientations. It appears noteworthy to mention that both a microfibrillar component and a lamellar component are existing in the material from the beginning, and that a proceeding partition of the inclined bi-lamellae into fragments is already indicated during the initial process of elongation.

All the discussed changes in L (Figure 7) concern only measurements under stress. From ε = 140%, the scattering patterns taken in the absence of stress are of four-point type and the question is, if the material is built from tilted lamellae or from a macrolattice of microfibrils. The CDFs (Figure 9,10) exhibit the presence of bi-domains from tilted lamellae that support the model of zigzag lamellae.[5] With increasing reversing-deformation ε the tilt-angle is growing to 60° at $\varepsilon = 510\%$. The trend towards formation of zigzag assemblies of parallel lamellae is strongly enhanced when the sample is not loaded. It increases significantly as the reversing deformation in the straining cycle (ε = 200–510%) is increased (Figure 6, after ε = 200–510%, σ = 0). Simultaneously, the shape of the scattering patterns taken under stress at ε = 200–500% is closer to the lobe-type than to the four-point type. Such a difference between the scattering patterns suggests substantial morphological changes. These changes are clearly identified in the CDF (Figure 10). It shows in the strained state a disruption of tilted lamellae into smaller pieces. At $\varepsilon = 250\%$ the fragments have formed a macrolattice with hexagonal order. When the elongation is increased beyond that, the lattice is transformed into an ensemble of microfibrils with little correlation in lateral direction. From the CDF it is clearly deduced that the samples subjected to the highest deformations and thereafter unloaded consist of parallel crystalline lamellae tilted with respect to the fiber axis (FA). A zigzag shaped arrangement of these layers in lateral direction is, on the other hand, not discernible from the CDF. A simplified sketch of the basic states of nanostructure as extracted from the SAXS data is presented in Figure 11.

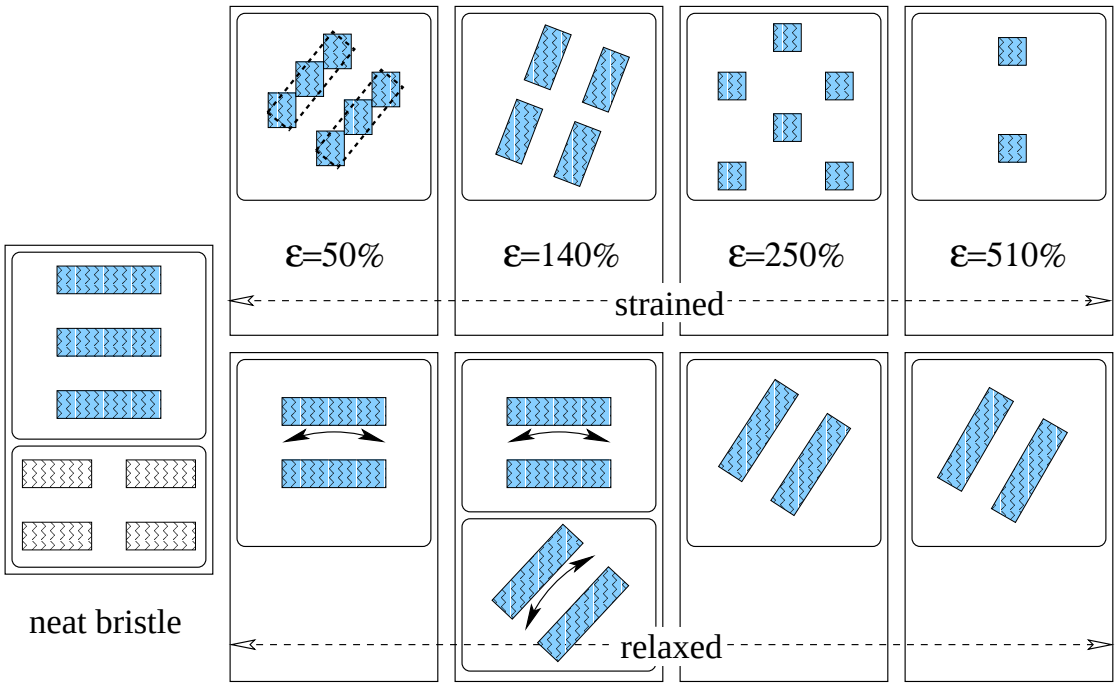

Figure 11: Arnitel® EM400 bristle nanostructure as a function of elongation ε in the elongated (top) and the relaxed (bottom) state, respectively. A microfibrillar structure always present (like the one outlined in the top right cartoon) is never sketched. A less simplified and more probable view of the tilted lamellae is indicated at $\varepsilon = 50\%$

If really filled lamellae or only assemblies of blocks are observed cannot be deduced from the presented scattering data. In the latter case a rotation of a lamella could be performed by a more probable process of progressive displacement of adjacent blocks in straining direction.

It is important here to emphasize that for the nanostructure at low and medium elongation: (i) the proximate morphology and the described morphological transition between inclined lamellar assemblies and flat ones is completely reversible; (ii) the trend to the formation of zigzag morphologies (or, the increase of the inclination to the fiber axis in the case of the unloaded samples) strongly grows with the progress of the macrodeformation ε. It can be assumed that such reversible morphological transition contributes to the formation of the elastic properties of thermoplastic elastomers as was suggested previously.[5]

One can assume that the considerable number of molecules connecting parallel lamellae causes a better-coordinated response to the changes of stress and/or of strain. The interfibrillar tie molecules holding together the crystalline domains of neighboring microfibrils are responsible for the more or less smooth distribution of the external stress in the sample. Taking into account the larger amount of amorphous material in the interfibrillar regions than that within the fibrils,[3] the creation of new tie molecules appears more probable to happen in the phase surrounding the microfibrils, than in the amorphous regions from inside the microfibrils.

Conclusions

By performing SAXS measurements during the progressive elongation of some polyesters and poly(ether esters) samples containing glycols with varying length, it was found that the extensibility strongly depends on the flexibility of the glycol residues. It increases from 10% (PET) to 510% (for a commercial PEE Arnitel® EM400).

Studying the relationship between the macro- (or, the external deformation denoted by ε) and the microdeformation expressed by the change of the long spacing L, in accordance with previous observations it was established that three typical deformational ranges exist. Within the lowest deformation range (up to 10% for PBT and 80% for PEE), the deformation obeys the affine model and is due to conformational changes occurring only in the amorphous intercrystalline areas. In the next deformation range (80–140%), observable for the PEE samples only, a second periodicity appears as a result of relaxation of a part of the microfibrils owing to a loss of microfibrillar contacts at this level of deformation. Finally, within the third deformational range of PEE (between 140 and 510%), four-point scattering patterns appear when the measurements are performed after removing the stress. Two-point diagrams characterize all measurements under stress. Using the multidimensional chord distribution function (CDF) analysis it was verified that the two-point diagram results from sets of parallel lamellar stacks, being perpendicular to the stretching direction, the four-point diagram is related to stacks of layers, tilted with respect to the longitudinal direction (fiber axis). The transition from one to the other type of lamellar arrangement is reversible. It is believed that this reversibility on morphological level contributes to the deformation reversibility of the thermoplastic materials.

Acknowledgment: This investigation was supported by the Bilateral Cooperation Program between the *University of Hamburg*, Germany, and the *University of Sofia*, Bulgaria, which is funded by the *DAAD*. SAXS investigations were supported by *HASYLAB*, Hamburg under project II-01-41. One of us (S.F.) expresses his warmest thanks to the *Alexander-von-Humboldt Foundation* for the "Humboldt Research Award" enabling the finalization of this study. The authors thank Dr. *D. Sapoundjieva* for her help during X-ray measurements.

Received: November 7, 2002
Revised: March 9, 2003
Accepted: March 11, 2003

References

[1] H. Schröder, R. G. Cella, in: H. F. Mark, N. M. Bikales, C. G. Overberger, G. M. Enges, Eds. "Encyclopedia of polymer science and engineering", John Wiley & Sons, New York, vol. 12, **1988** .
[2] R. N. Legge, G. Holden, H. Schröder, R. P. Quirk, Eds. *Thermoplastic Elastomers*, Hanser Publishers, Munich, Vienna, New York, 2nd edition, **1996**.
[3] S. Fakirov, C. Fakirov, E. W. Fischer, M. Stamm, *Polymer* **1991**, *32*, 1173.
[4] A. A. Apostolov, S. Fakirov, *J. Macromol. Sci. - Phys.* **1992**, *B31*, 329.
[5] S. Fakirov, C. Fakirov, E. W. Fischer, M. Stamm, A. A. Apostolov, *Colloid Polym. Sci.* **1993**, *271*, 811.
[6] Z. Denchev, M. Stamm, S. Fakirov, unpublished data.
[7] S. Fakirov, Z. Denchev, A. A. Apostolov, M. Stamm, C. Fakirov, *Colloid Polym. Sci.* **1994**, *272*, 1363.
[8] S. Fakirov, C. Fakirov, E. W. Fischer, M. Stamm, *Polymer* **1992**, *33*, 3818.
[9] N. Stribeck, D. Sapoundjieva, Z. Denchev, A. A. Apostolov, H. G. Zachmann, M. Stamm, S. Fakirov, *Macromolecules* **1997**, *30*, 1329.
[10] N. Stribeck, *ACS Symp. Ser.* **2000**, *739*, 41.
[11] N. Stribeck, *J. Appl. Cryst.* **2001**, *34*, 496.
[12] N. Stribeck, S. Fakirov, D. Sapoundjieva, *Macromolecules* **1999**, *32*, 3368.
[13] N. Stribeck, S. Fakirov, *Macromolecules* **2001**, *34*, 7758.
[14] S. Fakirov, N. Stribeck, in: S. Fakirov, Ed. "Handbook of Thermoplastic Polyesters", Wiley-VCH, Weinheim, vol. 1, **2002** pp. 671–716.

[15] N. Stribeck, E. Buzdugan, P. Ghioca, S. Serban, R. Gehrke, *Macromol. Chem. Phys.* **2002**, *203*, 636.
[16] N. Stribeck, R. Bayer, G. von Krosigk, R. Gehrke, *Polymer* **2002**, *43*, 3779.
[17] C. G. Vonk, *Colloid Polym. Sci.* **1979**, *257*, 1021.
[18] W. Ruland, *Colloid Polym. Sci.* **1977**, *255*, 417.
[19] W. Ruland, *Colloid Polym. Sci.* **1978**, *256*, 932.
[20] N. Stribeck, W. Ruland, *J. Appl. Cryst.* **1978**, *11*, 535.
[21] J. Brandrup, E. H. Immergut, Eds. *Polymer Handbook*, Wiley Interscience, New York, Chicester, Brisbane, Toronto, Singapore, 3rd edition, **1989**.
[22] S. A. Zhurkov, A. I. Slutsker, A. A. Yastrebinski, *Dokl. Acad. Nauk SSSR* **1963**, *153*, 303; *Chem. Abstr. 60:6943d*.
[23] E. W. Fischer, S. Fakirov, *J. Mater. Sci.* **1976**, *11*, 1041.
[24] S. Fakirov, O. Samokovlijsky, N. Stribeck, A. A. Apostolov, Z. Denchev, D. Sapoundjieva, M. Evstatiev, A. Meyer, M. Stamm, *Macromolecules* **2001**, *34*, 3314.
[25] T. Pakula, K. Saijo, H. Kawai, T. Hashimoto, *Macromolecules* **1985**, *18*, 1294.
[26] V. I. Gerasimov, Y. V. Genin, A. I. Kitaigorodsky, D. Y. Tsvankin, *Colloid Polym. Sci.* **1972**, *250*, 518.